

## Numerical analysis of modal tomography for solar multi-conjugate adaptive optics

Bing Dong<sup>1</sup>, De-Qing Ren<sup>1,2</sup> and Xi Zhang<sup>2</sup>

<sup>1</sup> Physics & Astronomy Department, California State University Northridge, CA, 91330-8268, USA; [dongbing@rocketmail.com](mailto:dongbing@rocketmail.com)

<sup>2</sup> National Astronomical Observatories/Nanjing Institute of Astronomical Optics & Technology, Chinese Academy of Sciences, Nanjing 210042, China

Received 2011 August 20; accepted 2011 December 27

**Abstract** Multi-conjugate adaptive optics (MCAO) can considerably extend the corrected field of view with respect to classical adaptive optics, which will benefit solar observation in many aspects. In solar MCAO, the Sun structure is utilized to provide multiple guide stars and a modal tomography approach is adopted to implement three-dimensional wavefront restorations. The principle of modal tomography is briefly reviewed and a numerical simulation model is built with three equivalent turbulent layers and a different number of guide stars. Our simulation results show that at least six guide stars are required for an accurate wavefront reconstruction in the case of three layers, and only three guide stars are needed in the two layer case. Finally, eigenmode analysis results are given to reveal the singular modes that cannot be precisely retrieved in the tomography process.

**Key words:** instrumentation: multi-conjugate adaptive optics — tomography

### 1 INTRODUCTION

Due to the anisoplanatism of atmospheric turbulence, a conventional adaptive optics system can only provide nearly diffraction-limited imaging within some arcseconds in the visible band. This narrow field of view (FOV) is insufficient for many applications. In solar observation, a sunspot has a size of typically 30 arcsec and the active regions often extend to 2–3 arcmin. Multi-conjugate adaptive optics (MCAO) is considered as the most promising technique to significantly increase the corrected FOV. This technique employs several deformable mirrors conjugated to different atmospheric layers to perform three dimensional wavefront error corrections. A key problem in MCAO is how to sense phase perturbations at different altitude layers. Two main concepts named “tomography” (Tallon & Foy 1990) and “layer oriented” approaches (Ragazzoni et al. 2002) have been proposed to deal with wavefront sensing issues in MCAO. Both of these methods have pros and cons and we will focus on the former in this paper.

The Sun is an ideal target to perform MCAO since a solar structure (sunspots, pores and granulation) can provide multiple “guide stars” in any desired configuration. We noticed that a tomography approach was generally used or tested for solar telescopes (Berkefeld et al. 2003, Langlois et al. 2004), which implied its good applicability and practicality for solar MCAO. In this paper, the

modal tomography approach is discussed in detail and related numerical simulations are performed to investigate the behavior of this algorithm. The simulation results are presented at the end.

## 2 PRINCIPLE OF MODAL TOMOGRAPHY

The principle of modal tomography was initially proposed by Ragazzoni (Ragazzoni et al. 1999). Here we suppose that  $N$  different guide stars are located properly on the sky and the atmospheric turbulence is restricted to  $M$  different altitude layers. The guide stars considered here are all natural guide stars obtained from solar structures so the cone effect and tip-tilt indetermination problems involved in laser guide star application are not taken into account. The wavefront of each guide star can be detected by a wavefront sensor and then be described by a finite number ( $p$ ) of Zernike modes suggested by Noll (1976), as

$$L_i = [a_2, a_3, \dots, a_{p+1}], \quad i = 1, 2, \dots, N, \quad (1)$$

where  $i$  is the running index of guide stars;  $L_i$  is the vector of Zernike coefficients of the wavefront coming from guide star  $i$ ;  $a$  denotes the Zernike coefficient. The piston term is omitted here since it cannot be measured by typical wavefront sensors.

The expansion of the wavefront coming from guide star  $i$  at layer  $j$  is defined as  $L_{ij}$ . The wavefront coming from guide star  $i$  can be computed by the wavefront integrated over all layers

$$L_i = \sum_{j=1}^M L_{ij}, \quad j = 1, 2, \dots, M, \quad (2)$$

where  $j$  is the running index of atmospheric layers. The circular region encompassing all guide star beams at each layer is the so-called metapupil. The modal expansion of the wavefront over the metapupil is given as  $W_j$ . The geometry of the footprints of guide stars and the metapupil is depicted in Figure 1.

Given the known geometry of these circular regions, one can get a set of matrix values  $A_{ij}$  providing the transformation from  $W_j$  to  $L_i$ .

$$L_i = \sum_{j=1}^M L_{ij} = \sum_{j=1}^M A_{ij} W_j. \quad (3)$$

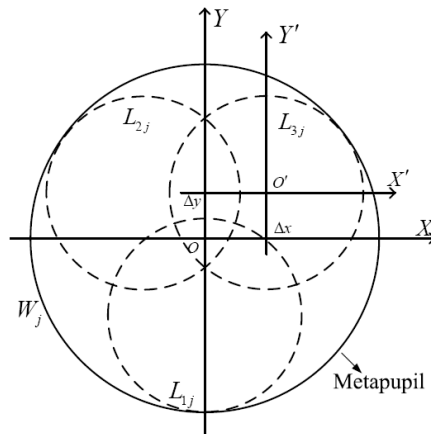


**Fig. 1** Relative position of three guide star footprints and the corresponding metapupil in the upper layer.

The wavefront of guide star  $i$  at layer  $j$  is restricted to a smaller circle with coordinate system  $O'X'Y'$  (Fig. 1) which has an origin shifted by  $\Delta x$  and  $\Delta y$  in  $OXY$  coordinates, and the unit length is  $k$  times smaller. The element of matrix  $A_{ij}$  with row number  $m$  and column number  $n$  can be calculated by

$$a_{mn} = \pi^{-1} \int Z_n(\Delta x + kx, \Delta y + ky) Z_m(x, y) dx dy, \quad (4)$$

where  $Z$  is the Zernike polynomial. According to Equation (3), the equation including all guide stars and perturbing layers is given as

$$\begin{bmatrix} L_1 \\ L_2 \\ \vdots \\ L_N \end{bmatrix} = \begin{bmatrix} A_{11} & A_{12} & \cdots & A_{1M} \\ A_{21} & A_{22} & \cdots & A_{2M} \\ \vdots & \vdots & \ddots & \vdots \\ A_{N1} & A_{N2} & \cdots & A_{NM} \end{bmatrix} \begin{bmatrix} W_1 \\ W_2 \\ \vdots \\ W_M \end{bmatrix} \quad (5)$$

which can be written in a compact form as

$$L = AW. \quad (6)$$

The tomographic matrix  $A$  is the link between Zernike modes of guide stars and those of metapupils. Provided  $N \geq M$  (i.e. the GS number is not less than the layer number), one can easily retrieve  $W$  using a singular value decomposition (SVD) method. Then vector  $W$  can be used to control deformable mirrors conjugated to turbulent layers.

$$W = A^+ L, \quad (7)$$

where  $A^+$  denotes the pseudo-inverse of matrix  $A$ .

### 3 MODEL DESCRIPTIONS

To simulate the process of modal tomography, phase screens on each layer should be generated first. Here we assume that the phase distributions in each layer follow Kolmogorov statistics. For a given seeing condition  $r_0$  (Fried's coherence length), a series of random Zernike coefficients can be generated by Karhunen-Loeve functions suggested by Roddier (1990). The atmospheric seeing of a certain layer with a thickness of  $h_i$  is calculated by

$$r_i = \left[ 0.423k^2 \sec(\gamma) \int_{h_i} C_n^2(h) dh \right]^{-3/5}, \quad i = 1, 2, \dots, M, \quad (8)$$

where  $C_n^2$  is the atmospheric structure constant,  $\gamma$  is the zenith angle and  $k = 2\pi/\lambda$ .

In our simulation,  $C_n^2$  is considered as the Hufnagel-Valley Boundary model (Eq. (9)) and the thicknesses of atmospheric layers are set as 1 km, which leads to a total  $r_0$  of 5 cm and an isoplanatic angle of 1.44 arcsec for the wavelength at 0.5  $\mu\text{m}$ . The size of the phase screens corresponds to a FOV of 80 arcsec and a telescope diameter of 1.5 m.

$$C_n^2(h) = 5.94 \times 10^{-23} h^{10} e^{-h} (21/27)^2 + 2.7 \times 10^{-16} e^{-2h/3} + 1.7 \times 10^{-14} e^{-10h}. \quad (9)$$

It has been demonstrated that whatever the true atmospheric profile is, only two or three equivalent layers are required for accurate restoration of the phase in the whole FOV (Fusco et al. 1999). In the following, two cases will be discussed: two layers located at 0 and 4 km and three layers at 0, 4 and 10 km respectively (Fig. 2). Figure 3 illustrates the footprints of different numbers of guide stars at the 4 km layer. The guide stars are situated at the vertices of a regular polygon inscribed in a circle with radius of 40 arcsec. An additional guide star is located on the axis if the number of guide stars is greater than three.

The wavefront related to each guide star is detected by a wavefront sensor such as a correlating Hartmann-Shack. We will not consider any measurement noise or undersampling error existing in real wavefront sensing so we can focus on the behavior of the tomography algorithm.

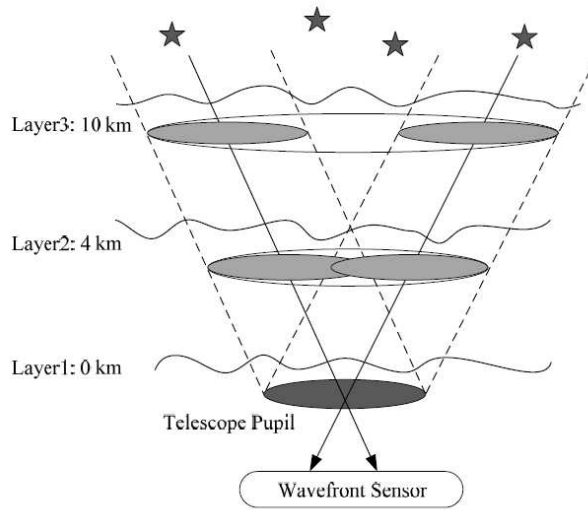


**Fig. 2** Scheme of modal tomography with three equivalent turbulent layers.

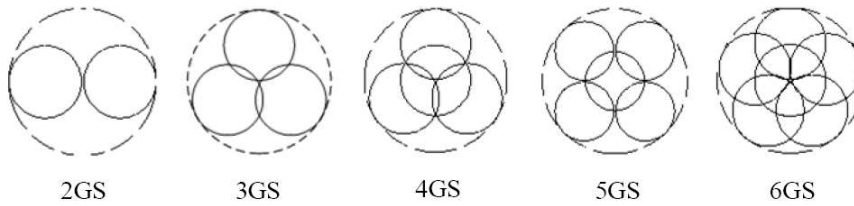


**Fig. 3** Geometrical views of different guide star beams through a layer at 4 km.

## 4 NUMERICAL ANALYSIS AND RESULTS

In our simulation, 100 groups of phase screens expanded with the first 36 Zernike polynomials are simulated for each configuration. For each data group, the variance of wavefront estimation error in each layer is given by

$$\sigma_i^2 = \frac{\iint [\hat{\varphi}_i(\rho, \theta) - \varphi_i(\rho, \theta)]^2 d\rho d\theta}{\iint \varphi_i(\rho, \theta) d\rho d\theta}, \quad i = 1, 2, \dots, M, \quad (10)$$

where  $\varphi$  is the simulated wavefront and  $\hat{\varphi}$  is the estimated wavefront. The tip/tilt terms are removed from both of them since they are corrected independently by a tip/tilt mirror. We can expect that the criteria  $1 - \langle \sigma_i \rangle$  can reflect the phase estimation accuracy, where  $\langle \rangle$  denotes the operation of averaging.

### 4.1 Two Layer Case

Typical results of wavefront estimation with two layers and different numbers of guide stars are illustrated in Figure 4. The wavefront estimation accuracy is given in Table 1. As shown in Table 1, at least three guide stars are required for accurate wavefront reconstruction.

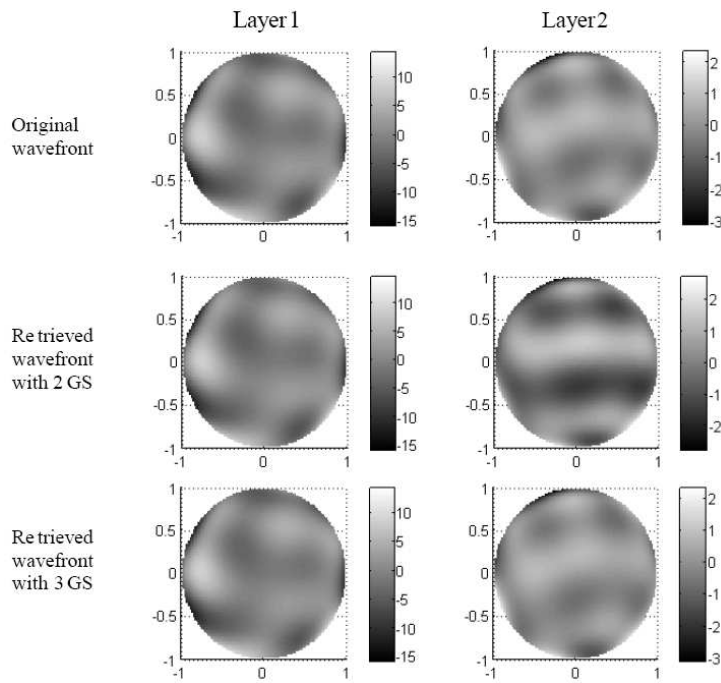


**Fig. 4** Wavefront estimation results with two layers and different numbers of guide stars. The wavefront maps are normalized in unit disks with the phase unit in radians.

**Table 1** Phase Estimation Accuracy for the Two Layer Case

Guide Star Number	Layer 1	Layer 2
2 GS	0.83	0.62
3 GS	1	1
4 GS	1	1

**Table 2** Phase Estimation Accuracy for the Three Layer Case

Guide Star Number	Layer 1	Layer 2	Layer 3
4 GS	0.97	0.76	0.65
5 GS	0.98	0.85	0.79
6 GS	1	1	1

## 4.2 Three Layer Case

Typical results of wavefront estimation with three layers and different numbers of guide stars are illustrated in Figure 5. The phase estimation accuracy for each configuration is given in Table 2. As shown in Table 2, the estimated wavefront is very similar to the original one at the ground layer (layer 1). With an increase in the layer's altitude, the phase estimation accuracy becomes worse. It is shown that at least six guide stars are required for accurate wavefront reconstruction in all three layers.

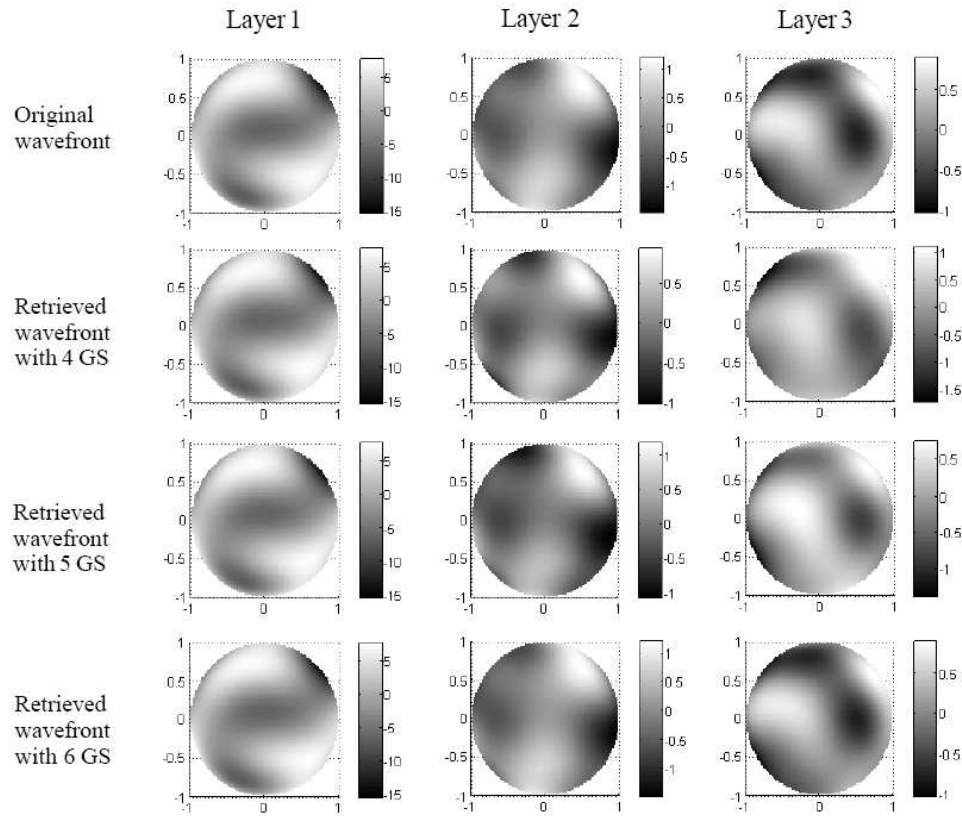


**Fig. 5** Wavefront estimation results with three layers and a different number of guide stars. The wavefront maps are normalized in unit disks with the phase unit in radians.

### 4.3 Eigenmode Analysis

As shown in Tables 1 and 2, there is a minimum number of guide stars required for accurate wavefront reconstruction. This phenomenon can be interpreted by eigenmode analysis of the tomography process (Louarn & Tallon 2002). Singular value decomposition is applied to the tomography matrix (i.e. matrix  $A$  in Eq. (6)) to obtain the singular modes in different system configurations. The singular modes defined here are some Zernike modes that cannot be accurately retrieved. Since the tomography matrix  $A$  is usually ill-conditioned, some eigenvalues of matrix  $A$  will be zero, which correspond to singular modes of the system. The singular modes for two layers and three layers are summarized in Table 3 and Table 4 respectively.

**Table 3** Singular Modes for Two Layer Tomography

Guide Star Number	Singular Zernike Modes
2 GS	$Z_1 - Z_{21}$
3 GS	$Z_1$ (piston), $Z_2$ (tip), $Z_3$ (tilt)
4 GS	$Z_1$ (piston), $Z_2$ (tip), $Z_3$ (tilt)

**Table 4** Singular Modes for Three Layer Tomography

Guide Star Number	Singular Zernike Modes
4 GS	$Z_1$ (piston), $Z_2$ (tip), $Z_3$ (tilt), $Z_4$ (defocus), $Z_5$ ( $y$ -astigmatism), $Z_6$ ( $x$ -astigmatism), $Z_9$ ( $y$ -trefoil)
5 GS	$Z_1$ (piston), $Z_2$ (tip), $Z_3$ (tilt), $Z_4$ (defocus), $Z_6$ ( $x$ -astigmatism)
6 GS	$Z_1$ (piston), $Z_2$ (tip), $Z_3$ (tilt)

Tables 3 and 4 illustrate that the first three terms (piston, tip and tilt) are always singular. This is because the piston and tip/tilt errors at different layers can be compensated for each other so they cannot be localized to the layer where they are produced. If the number of guide stars is not enough, the wavefront at a higher altitude is undersampled so more singular modes will appear.

## 5 CONCLUSIONS

Solar telescopes can benefit from MCAO to obtain a large observing FOV. Modal tomography is an efficient way to get the phase distribution of the turbulence volume. A numerical simulation model was built to investigate the behavior of the modal tomography algorithm with a different number of guide stars. Simulation results show that at least six guide stars are required for an accurate wavefront reconstruction in the case of three layers and only three guide stars are needed for the two layer case. Singular modes in the tomographic process can be obtained by means of eigenmode analysis which interprets the guide star requirement in the tomography algorithm.

## References

- Berkefeld, T., Soltau, D., & von der Lühe, O. 2003, in Society of Photo-Optical Instrumentation Engineers (SPIE) Conference Series 4839, Adaptive Optical System Technologies II, eds. P. L. Wizinowich, & D. Bonaccini (Waikoloa: SPIE), 544
- Fusco, T., Conan, J.-M., Michau, V., Mugnier, L. M., & Rousset, G. 1999, *Optics Letters*, 24, 1472
- Langlois, M., Moretto, G., Richards, K., Hegwer, S., & Rimmele, T. R. 2004, in Society of Photo-Optical Instrumentation Engineers (SPIE) Conference Series 5490, Advancements in Adaptive Optics, eds. D. Bonaccini Calia, B. L. Ellerbroek, & R. Ragazzoni (Bellingham: SPIE), 59
- Louarn, M. L., & Tallon, M. 2002, *Journal of the Optical Society of America A*, 19, 912
- Noll, R. J. 1976, *Journal of the Optical Society of America (1917–1983)*, 66, 207
- Ragazzoni, R., Diolaiti, E., Farinato, J., et al. 2002, *A&A*, 396, 731
- Ragazzoni, R., Marchetti, E., & Rigaut, F. 1999, *A&A*, 342, L53
- Roddier, N. 1990, *Optical Engineering*, 29, 1174
- Tallon, M., & Foy, R. 1990, *A&A*, 235, 549